

Abstract. An extended radio emission after a soft X-ray (SXR) maximum was detected in the active region NOAA 9077 by several observatories for the solar flare after 21:42 UT on July 10, 2000. Also some radio fine structures before the enduring radio emission were observed with the 1.0-2.0 GHz spectrometer of Beijing Astronomical Observatory (BAO) in the same time. We apply a shear-driven quadrupolar reconnection model (SQR) to analyze the fine structures and the related radio emission. We find that the footpoint shear motion of the flux loop is accompanied with the emerging up of the loop during the reconnection process. We tentatively interpret the extended radio emission as the nonthermal radiation caused by a new reconnection process between emerging flux loop and pre-existing overarching loop after the soft X-ray maximum.

Key words: Sun: flare – Sun: radio radiations

Extended radio emission after the soft X-ray maximum of the NOAA 9077 AR solar flare on July 10, 2000

Shujuan Wang^{1,2}, Yihua Yan^{1,2}, and Qijun Fu^{1,2}

¹ Beijing Astronomical Observatory, Chinese Academy of Sciences, Beijing 100012, China

² National Astronomical Observatories, Chinese Academy of Sciences, Beijing 100012, China

Received xxx/Accepted xxx

1. Introduction

It is widely accepted that the nonthermal radio burst emission should take place *before* the thermal SXR maximum, for the basic process is thought to be the following: first, high-energy particles are accelerated during a reconnection of magnetic flux and propagate along field lines, exciting the radio bursts; then, these particles pour down continuously, causing chromospheric evaporation, and increasing the SXR emission to its peak (Heyvaerts et al. 1977; Mclean & Labrum 1985).

However, an event of extended nonthermal emission *after* the thermal maximum has been detected by several observatories on July 10, 2000. This event seems to suggest that the extended nonthermal radiation resulted from repeated triggering of a new magnetic reconnection. There are two different ways to interpret the triggering. In the emerging flux model (Heyvaerts et al. 1977), when the magnetic flux loops emerge from below the photosphere and interact with the overlying field, continuous reconnection occurs in the current sheet between the new and old fluxes. In the SQR model (Aschwanden 1998), the shear motion of the footpoint will cause the magnetic field between the sheared small-scale loop and the overlying unsheared large-scale loop to become increasingly sheared and compressed, triggering quadrupolar X-type reconnection. The latter interpretation also regards, as a consequence of the reconnection, the various radio fine structures, including type III, and U bursts, and reverse-slope (RS)-drifting bursts. Indeed, some such radio fine structures were observed with the 1.0-2.0 GHz spectrometer of BAO in the event on July 10, 2000.

This Letter first presents the observations of the event. Then we use the SQR model to analyze the radio fine structures and the related broadband radio bursts. We find that both the shear motion and emerging motion play a part during the magnetic reconnection for this event.

Table 1. Data of the radio burst radiations and SXR burst

Begin (UT)	Max (UT)	End (UT)	Obs.	Type	Range (MHz)	Imp. (sfu)
2121	2208	2314	PALE	RBR	245	13000
2117	2205	2308	PALE	RBR	410	7200
2117	2207	2254	PALE	RBR	606	1200
2158E	2213	2249	BAO	RBR	2840	3085
2117	2210	2257	PALE	RBR	15400	2600
2105	2142	2227	GOES8	XRb	1-8Å	M5.7

2. Observations

The observations of PALE (Palehua station) and GOES 8 were prepared by Space Environment Center (SEC) on the internet. The other observations were made with the 1.0-2.0 GHz solar radio fast dynamic spectrometer and the 2.84 GHz radio telescope at Huairou Solar Observing Station of BAO (Fu et al. 1995).

The July 10, 2000 flare, classified as M5.7/2B, was observed at 21:05-22:27 UT in Active Region 9077 at position N19E49. Maximum was at 21:42 UT. Morphologically, the flare was a two-ribbon flare. The peak flux density at 2695 MHz was 140 sfu at 21:27 UT before the SXR maximum (by SEC). However an extended and very strong radio emission (up to 3085 sfu at 2840 MHz) was detected after 21:42 UT, and continued to about 23:00 UT, by several observatories. The data are summarized in Table 1. It indicates repeated occurrence of magnetic reconnection.

A group of radio fine structures before the broadband radio bursts were observed in the range of 1.0-2.0 GHz 21:59:30-22:00:10 UT (Fig. 1). Fig. 2 shows the GOES 8 SXR data between 21:00 and 22:30 UT. Our radio data at the several frequencies, which did not begin until 21:58 UT, are displayed in the inset, and are further blown up in the grey-scale picture below. The observed features can be summarized as follows.

(1) The fine structures contained four quasi-periods, the first one about 6 s between 21:59:32-21:59:38 UT, the second about 9 s between 21:59:38-21:59:47 UT, the third about 4 s between 21:59:47-21:59:52 UT, and the fourth

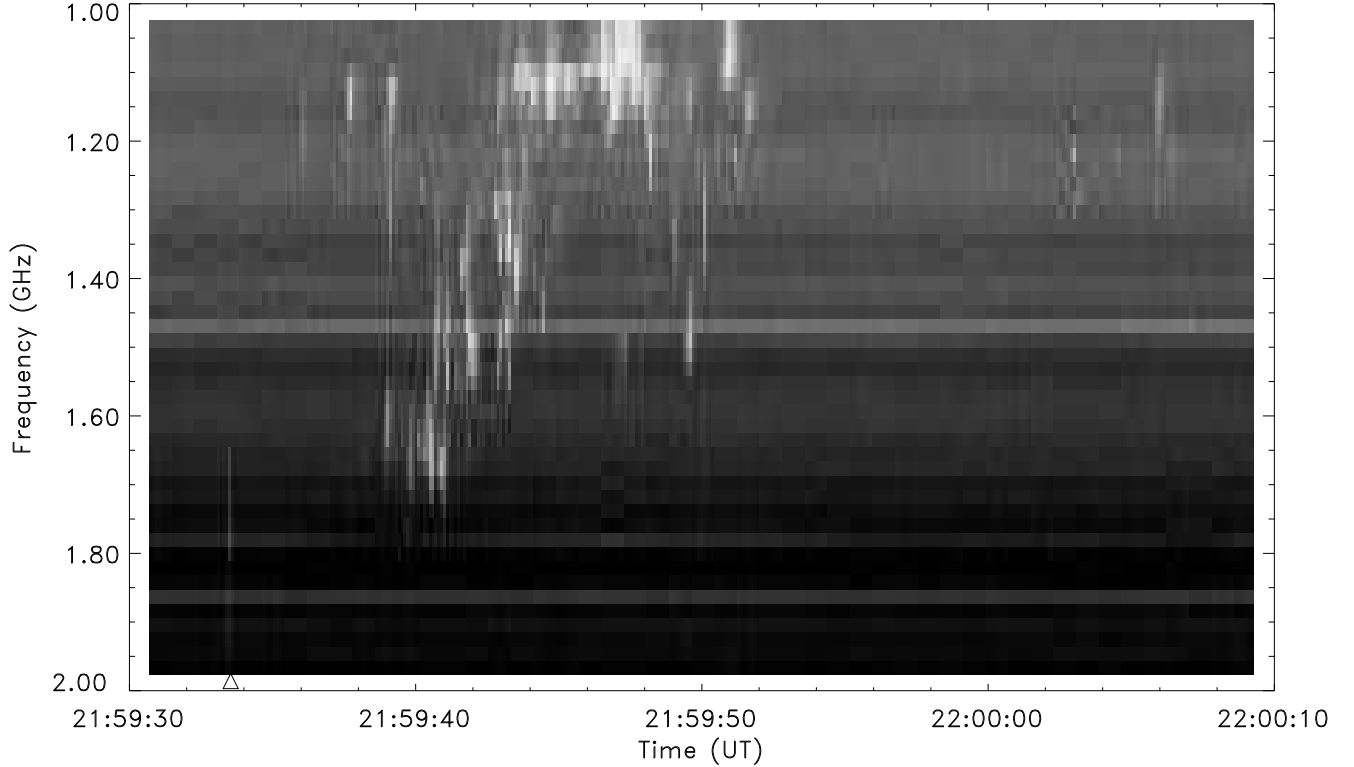


Fig. 1. Gray-scale plot of the fine structures of the radio bursts on July 10, 2000 observed by BAO. Enhanced flux shown bright. The sign “ Δ ” marks a very faint burst.

about 14 s between 21:59:52–22:00:05 UT. The average period was about 6.5 s.

(2) Each period included both type U and type RS bursts. The type U bursts occurred in the lower frequency range, and the type RS bursts, in the higher frequency range. All the type U bursts had a similar turnover frequency of 1.16 GHz.

(3) In each period, the flux density of the type U bursts was 3–4 times stronger than the type RS bursts.

(4) The average frequency drift rate of the type U bursts was about 100 MHz s^{-1} (both positive and negative), and that of the type RS bursts was about 800 MHz s^{-1} (negative). The former was clearly lower.

(5) The central frequencies of the type RS bursts drifted fast towards the lower frequency. The rate of drift decreased in time in the range $100\text{--}40 \text{ MHz s}^{-1}$.

(6) The type U bursts occurred after the type RS bursts.

(7) At 22:04 UT, some 4 minutes after the fine structures, a broadband radio burst appeared, which lasted until 22:49 UT.

3. Theoretical analysis

3.1. SQR model

According to Aschwanden (1998, Fig. 1 of his paper), the SQR model may contain the following process. Recognizing that shear motion along a neutral line to be an important condition for flaring, a consequence of a shear motion of the footpoint along the neutral line is that the magnetic field between the top of the sheared small-scale loop and the overlying unshaped large-scale field becomes increasingly sheared and compressed. At some point the rising sheared loop will intersect with the unshaped large-scale loop and trigger a quadrupolar X-type reconnection. During the reconnection, the connectivity of the field lines switches by exchanging the polarities of equal signs. The newly configured field lines then slip back from the X-point and relax to two dipole-like field lines. Then with the curvature of the magnetic field reduced, magnetic energy will be released (Aschwanden 1998, Aschwanden et al. 1999).

3.2. Radio bursts

As shown in Fig. 3, upward propagating electron beams, along open and closed field lines, can be detected in the form of Type III, J and U bursts; while downward propagating electron beams are detectable in the form of RS

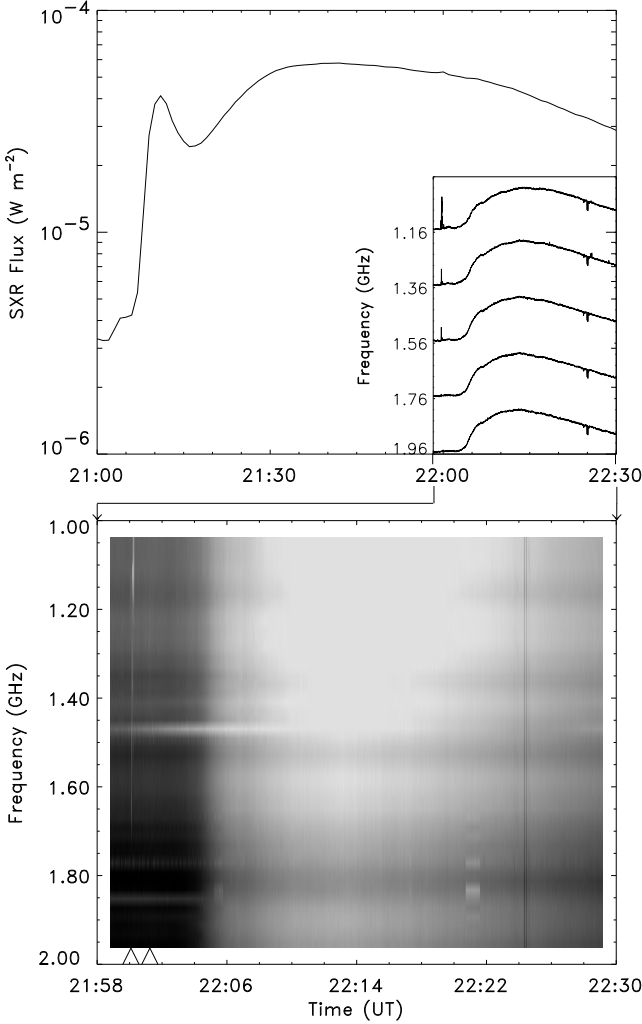


Fig. 2. Comparison of the SXR emission with the related radio bursts. *Top:* time profiles of the SXR flux (GOES 8) (*large*) between 21:00–22:30 UT, and of the related radio emission (*small*) after 21:58 UT (no data being available before 21:58 UT in BAO). *Bottom:* blow-up gray-scale plot of the radio emission in the range of 1.0–2.0 GHz. The radio fine structures corresponding to Fig. 1 are the bright lines before 22:01 UT marked with double “Δ”.

bursts. Therefore type U bursts occur in the lower frequency range while type RS bursts occur in the higher. The following expected observational signature can also be seen in Fig. 3: a quasi-periodic sequence of type U bursts with similar turnover frequencies produced by the upward propagating electron beams (Aschwanden 1998). The observational properties (1) and (2) in Sect. 2 are in agreement with the theoretical predictions here.

According to Zhao et al. (1997), if we assume the magnetic field of the active region to be a dipole field above the photosphere, then the relation between the height of

radio source (H) and its frequency (f) can be estimated by

$$H = d \left[\left(\frac{5.6 B_0}{f \text{ (MHz)}} \right)^{1/3} - 1 \right]. \quad (1)$$

Where the depth of the dipole field d is about 3.5×10^4 km, and B_0 is the magnetic field strength of the photosphere. For this event B_0 was about 2500 G (Huairou Station, BAO). Using the turnover frequency of 1.16 GHz, the height of the top of the unshered large-scale loop can be estimated to be about 4.5×10^4 km.

Upward-accelerated electrons encounter a decreasing magnetic field, which has a focusing effect on the pitch-angle distribution of the beam and makes it more prone to plasma emission. Also, the lower density encountered in upward direction makes it easier for plasma emission to escape. These two properties may be the main reason why upward propagating electron beams are detected much more frequently (type U bursts etc.) than downward beams (RS bursts) (Aschwanden 1998). Therefore, when the upward and downward beams are both detected in radio, the flux density of type U bursts can be stronger than the related type RS bursts. This agrees with observational property (3) in Sect. 2.

As the name implies, the large-scale loop have generally a much larger size than the small-scale loop: the typical height is 1.3×10^5 km for the former and 2.0×10^4 km for the latter (Aschwanden et al. 1992). The upward velocity of the electrons along the large-scale loop, then, is less than the downward velocity along the small-scale loop. Thus, the frequency drift rate of type U bursts is lower than that of type RS, as was stated under (4) in Sect. 2. According to Eq. 1, the spatial range (ΔH) can be obtained for each of the type U and RS bursts. Dividing ΔH by the corresponding time interval, we can obtain the electron velocity for each burst. The average upward and downward electron velocities were estimated to be of 1.8×10^3 km s⁻¹ and 1.4×10^4 km s⁻¹, respectively.

From the observational data, the central frequency (cf. the observed feature (5) in Sect. 2) of each RS burst can be obtained. Substituting the central frequency into Eq. 1, the corresponding height (H_c) can be estimated for each RS burst. We found H_c increased in time. This indicates that the small-scale loop was emerging from below. In the first period the velocity of emerging was faster, but it gradually slowed down in the three succeeding periods (cf. Feature (1) in Sect. 2). Typical emerging velocity during the second period is estimated at about 1500 km s⁻¹. Thus, besides the shear motion of the footpoint, which has been emphasized in the SQR model, there is the emerging motion of small-scale magnetic loop taking place in the course of the reconnection.

It was also expected from the SQR model that for a large flare the reconnection will continue for a long time; for example, lasting more than 3 minutes for the 1994-Jan-06 0405 flare (Aschwanden 1998). In this event, the flare

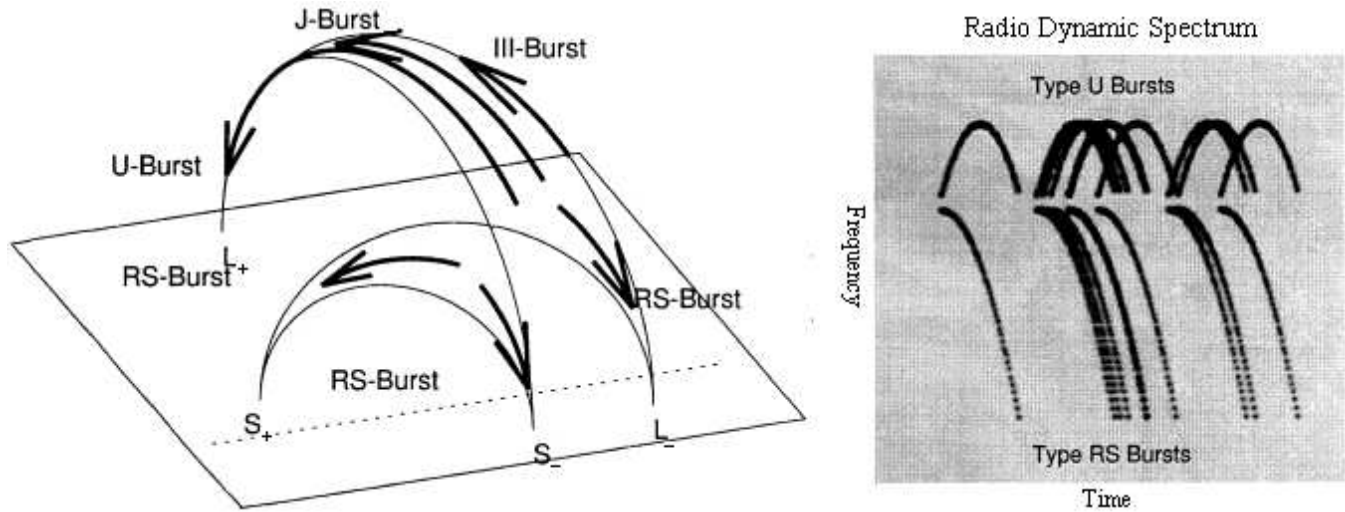


Fig. 3. Spatial trajectories of radio bursts in the SQR model (left frame) and the corresponding radio dynamic spectrum (right frame). A quasi-periodic sequence of acceleration episodes produces synchronized electron beams moving upwards (Type III, J and U bursts) and downwards (RS bursts) (Aschwanden 1998).

was a large flare (two-ribbon flare). Moreover the broadband radio bursts are believed to be the result of thermal bremsstrahlung from the hot and dense plasma that remains in the low corona even for some tens of minutes (Dulk 1985). Thus we can understand the reason why the broadband radio bursts appeared after the fine structures for about 4 minutes.

4. Discussion and Conclusions

Several conclusions can be drawn from the present study:

- (1) The extended radio emission was indeed caused by a new magnetic reconnection process.
- (2) There was a flux loop emerging from the below. Typical emerging velocity was about 1500 km s^{-1} .
- (3) Either the shear motion or the emerging motion or both could have triggered the quasi-periodic magnetic reconnection.
- (4) The radio fine structures provide clues for the understanding of the process of energy release in the initial phase of the flare.

The original SQR model only considered the shear motion as the trigger of the magnetic reconnection, but not the emerging motion. However the emerging motion was indeed reflected in the present observations. The model may thus be improved in the future. Besides, the type U bursts occurred after the type RS bursts, and the delay between the two tended to get shorter. This property may have something to do with the emerging motion, because the consequence of the small-scale loop emerging is that the tops of the two loops eventually reach the same height.

Acknowledgements. This research was supported by the National Nature Science Foundation of China under grant No. 19773016 and No. 19973008, and by Ministry of Science and Technology of China under grant No. G2000078403. We wish to

thank the anonymous referee for advice on the improvement of the Letter. We are also grateful to Dr T. Kiang for his revision on the language of the Letter.

References

- Aschwanden, M. J., Bastian, T. S., Benz, A. O., Brosius, J. W., 1992, ApJ 391, 380
- Aschwanden, M. J., 1998, Solar Physics with Radio Observations, Proceedings of Nobeyama Symposium 1998, NRO Report 479, 307
- Aschwanden, M. J., Kosugi, T., Hanaoka, Y., et al., 1999, ApJ 526, 1026
- Dulk, G. A., 1985, ARA&A 23, 169
- Fu, Q. J., Qin, Z. H., Ji, H. R., et al., 1995, Solar Phys. 160, 97
- Heyvaerts, J., Priest, E. R., Rust, D. M., 1977, ApJ 216, 123
- Mclean, D. J., Labrum, N. R., 1985, Solar Radiophysics, Cambridge Univ. Press, Cambridge, UK
- Zhao, R. Y., Jin, S. Z., Fu, Q. J., 1997, Solar Radio Microwave Bursts, Scientific Publishing House, Beijing, China